JACC: CARDIOVASCULAR IMAGING VOL. 3, NO. 8, 2010

ISSN 1936-878X/$36.00
PUBLISHED BY ELSEVIER INC. DOI:10.1016/j.jcmg.2010.06.004

Increased Glucose Uptake in Visceral Versus Subcutaneous Adipose Tissue Revealed by PET Imaging

Thomas Christen, MD, PhD,* Yuri Sheikine, MD, PhD,†‡ Viviane Z. Rocha, MD,* Shelley Hurwitz, PhD,§ Allison B. Goldfine, MD,‖ Marcelo Di Carli, MD,*†‡ Peter Libby, MD*

Boston, Massachusetts

OBJECTIVES The current study tested the hypothesis that glucose utilization differs between visceral adipose tissue (VAT) and subcutaneous adipose tissue (SAT), and investigated potential mechanisms for such a finding.

BACKGROUND VAT burden correlates better with cardiovascular risk than does SAT burden. Beyond volumetric measurement, glucose uptake in adipose tissue (AT) might reflect metabolic activity and provide pathophysiologic insight and aid risk stratification.

METHODS We retrospectively studied tissue-specific glucose uptake in vivo in clinically obtained whole-body fluorodeoxyglucose positron emission tomography (FDG-PET) scans in humans. We also assessed glucose uptake in vitro, using stromal vascular cells isolated from SAT and VAT of diet-induced obese C57BL/6 mice. Quantitative polymerase chain reaction (PCR) evaluated the expression of multiple genes involved in cellular glucose metabolism, including glucose transporters (GLUT-1, -3, and -4) and hexokinases (HK-1 and -2) in SAT and VAT of obese C57BL/6 mice.

RESULTS We analyzed whole-body FDG-PET scans from 31 obese and 26 lean patients. VAT exhibited higher FDG uptake compared with SAT ($p < 0.0001$) independent of age, sex, body mass index, comorbidities, and medications. To investigate mechanisms underlying this observation, we studied glucose uptake in the stromal vascular cell fraction of AT, which is rich in inflammatory cells. Stromal vascular cells from VAT of diet-induced obese C57BL/6 mice exhibited higher glucose uptake than those from SAT ($p = 0.01$). Evaluation of expression of glucose transporters (GLUT-1, -3, and -4) and hexokinases (HK-1 and -2), revealed increased expression of HK-1 in VAT-derived compared with SAT-derived stromal vascular cells, and also in visceral versus subcutaneous unfractionated AT.

CONCLUSIONS In humans in vivo, VAT has increased glucose uptake compared with SAT, as determined noninvasively with FDG PET imaging. Differential stromal metabolic activity may be 1 mechanism underlying differences in metabolic activity of visceral and subcutaneous AT. (J Am Coll Cardiol Img 2010;3:843–51) © 2010 by the American College of Cardiology Foundation

From the *Division of Cardiovascular Medicine, Brigham and Women's Hospital, Boston, Massachusetts, †Division of Nuclear Medicine and Molecular Imaging, Department of Radiology, Brigham and Women's Hospital, Boston, Massachusetts, ‡Noninvasive Cardiovascular Imaging Program, Departments of Medicine (Cardiology) and Radiology, Brigham and Women's Hospital, Boston, Massachusetts, §Department of Medicine, Brigham and Women's Hospital, Boston, Massachusetts; and the ‖Joslin Diabetes Center, Harvard Medical School, Boston, Massachusetts. This work was funded in part by the Donald W. Reynolds Foundation, Translational Program of Excellence in Nanotechnology grant U01HL080731. Drs. Christen, Sheikine, and Rocha contributed equally to this study. An alternative spelling of Dr. Sheikine's name is Yury Sheykin.

Manuscript received January 25, 2010; revised manuscript received June 10, 2010, accepted June 10, 2010.

JACC: CARDIOVASCULAR IMAGING, VOL. 3, NO. 8, 2010
AUGUST 2010:843–51

The dramatic increase in obesity and related metabolic complications during the last decade threatens to reverse the progressive decrease in cardiovascular deaths realized over the last 50 years (1). Although excess overall adiposity associates with cardiovascular morbidity and mortality, the distribution of body fat across different adipose tissue

See page 852

(AT) compartments provides additional important information on risk (2,3). Indeed, whereas the amount of visceral adipose tissue (VAT) correlates highly with an adverse risk factor profile (4,5), the amount of subcutaneous adipose tissue (SAT) has a less ominous import in obese individuals (6).

The potential clinical impact of biologic diversity between fat depots has triggered intense research to better understand physiologic and molecular differences based on AT location. Several studies have already demonstrated differences between VAT and SAT regarding secretion of inflammatory mediators, gene expression, and cell morphology. Yet glucose utilization between these 2 adipose compartments remains incompletely understood (7–10). A recent study shows that AT glucose uptake determined by fluorodeoxyglucose positron emission tomography (FDG-PET) may complement volumetric measurements of fat for the purpose of risk estimation (11).

This study demonstrates higher FDG uptake in VAT compared with SAT in humans using the FDG-PET imaging technique, and investigates potential molecular mechanisms mediating this effect.

ABBREVIATIONS AND ACRONYMS

AT = adipose tissue
BMI = body mass index
CT = computed tomography
FDG = fluorodeoxyglucose
GLUT = glucose transporter
HK = hexokinase
PET = positron emission tomography
qPCR = quantitative polymerase chain reaction
SAT = subcutaneous adipose tissue
SUV = standard uptake value
SVC = stromal vascular cell
VAT = visceral adipose tissue
VOI = volume of interest

METHODS

Human subjects and FDG-PET imaging. The institutional review board of Brigham and Women's Hospital approved the human studies. We retrospectively analyzed 31 obese patients and 26 lean patients who underwent whole-body PET-computed tomography (CT) scanning for diagnosis or staging of primary lung cancer with respect to the intensity of FDG uptake in abdominal visceral and subcutaneous AT. Individuals exhibiting abnormal FDG uptake in the abdominal region suspicious for metastases, and 2 individuals with fat standard uptake values (SUVs) that were 8 and 18 standard deviations above the mean, were excluded from analysis. After fasting for 4 to 6 h, the patients received FDG (777 ± 111 MBq, 21 ± 3 mCi) intravenously, and whole-body images were acquired on a Discovery ST PET/CT scanner (General Electric, Milwaukee, Wisconsin), 83 ± 22 min after tracer administration as described previously (12). Briefly, a noncontrast CT scan was performed first for attenuation correction and localization. Immediately after the CT scan, the PET scan was acquired in 2-dimensional mode at 6 to 7 bed positions (4 min for each position). PET data were reconstructed using an ordered-subset expectation maximization iterative algorithm.

Hermes Gold 2.1 software (Hermes Medical Solutions, Stockholm, Sweden) was used for image analysis (Fig. 1). We first created a "fat mask" of the original CT image set by removing pixels with densities below −110 HU or above −70 HU, a range corresponding to AT densities in human subjects (13). We then divided the obtained CT fat mask by itself to acquire a binary CT fat mask in which pixels had the value of 1 in AT and 0 in all other tissues. We further resampled the original PET file to match the slice thickness and matrix size of the CT file, and multiplied the resampled PET image set by the binary CT fat mask. This operation left only those pixels in the PET image set that corresponded to the pixels with the value of 1 in the CT fat mask. We converted this PET image set into the original matrix size and proceeded with the analysis as follows. We drew regions of interest in visceral and subcutaneous AT in 15 to 25 consecutive slices to create a volume of interest (VOI). We recorded tracer activity (becquerels per cubic centimeter) in each pixel displaying a value above 0, and converted this number to the SUV using a standard formula accounting for pixel activity (becquerels per cubic centimeter), patient weight (kilograms), and injected dose (becquerels), decay corrected to the time of injection. We then averaged SUVs from each pixel in a VOI to obtain a single SUV for a given VOI in both SAT and VAT regions.

Experimental animals and isolation of stromal vascular cells. C57BL/6 mice were obtained from the Jackson Laboratory (Bar Harbor, Maine) and kept at a barrier animal facility of the Harvard Medical School. All experiments conformed to animal care protocols approved by the institutional review board. Mice were fed a high-fat diet (PicoLab Rodent Chow D12108, containing 40% kcal from fat, 1.25% cholesterol, 0% cholate; Research Diets, Inc., New Brunswick, New Jersey). At sacrifice, we

perfused animals with normal saline to remove blood cells from the vascular system and dissected abdominal subcutaneous and periepididymal visceral fat pads.

To isolate stromal vascular cells (SVCs), we minced the fat pads in phosphate-buffered saline (PBS) containing 2% bovine serum albumin and 250 U/ml of collagenase II (Worthington Biochemical Corporation, Lakewood, New Jersey), and incubated it at 37°C for 1 h. We passed the digested tissue through a 70-μm nylon cell strainer (BD Biosciences, San Jose, California) and centrifuged the flow-through. After removing the supernatant, we lysed red blood cells with ACK lysis buffer (Gibco, Carlsbad, California) and washed and counted the remaining cells, which we then used for cell culture or RNA isolation, as described in the following text.

Cytokines and chemicals. Murine cytokines were obtained from Peprotech (Rocky Hill, New Jersey) and tested by the manufacturer for the absence of lipopolysaccharide (LPS). We prepared all cytokine stock solutions in LPS-free sterile PBS and diluted the working solutions with culture medium before stimulation. Specific biological activities of cytokines were 1×10^7 U/mg for IFN-gamma, 1×10^7 U/mg for TNF-alpha, and 5×10^8 U/mg for IL-1beta. We describe cytokine concentrations in sections detailing cell stimulations. We purchased 2-deoxy-D-glucose (2dG) and cytochalasin B from Sigma (St. Louis, Missouri), and 3H-2dG from PerkinElmer (Waltham, Maine).

Glucose uptake assay. Cultured SVCs were incubated in KRH buffer (136 mmol/l NaCl, 4.7 mmol/l KCl, 1.25 mmol/l $MgSO_4$, 1.25 mmol/l $CaCl_2$, 50 mmol/l HEPES) for 30 min at 37°C to deplete endogenous glucose stores. Next, we added 3H-2dG and unlabeled 2dG to the cells (final concentration, 100 μmol/l for each, and specific activity of 0.5 μCi/sample for 3H-2dG) with or without the inhibitor cytochalasin B (final concentration 10 μmol/l) to determine carrier-nonspecific uptake (14). We incubated cells for 5 min at room temperature, after which we removed the incubation buffer and washed the cells twice with 25 mmol/l ice-cold unlabeled D-glucose to stop uptake of radiolabeled glucose via saturation of transporters. We lysed cells with 1% Triton X-100 (Sigma). We used lysates for liquid scintillation counting (Beckman LS 6000IC counter) and protein measurements using BCA assay (Pierce, Rockford, Illinois). The net uptake of 3H-2dG by cells is normalized to protein content and expressed as nanomoles of glucose per milligram of protein per minute. We analyzed each sample in duplicate, and the values were averaged. The data presented on the graphs and in the tables represent mean ± SEM of data obtained on cells from several experiments (n for each experiment is indicated in the respective figure legend). All graphs show GLUT-mediated glucose uptake (total uptake minus cytochalasin B-inhibited uptake).

Cell culture and stimulations. After isolation, we cultured murine SVCs in RPMI-1640 medium supplemented with 10% fetal calf serum (FCS), 100 U/ml penicillin, 100 μg/ml streptomycin, and 2

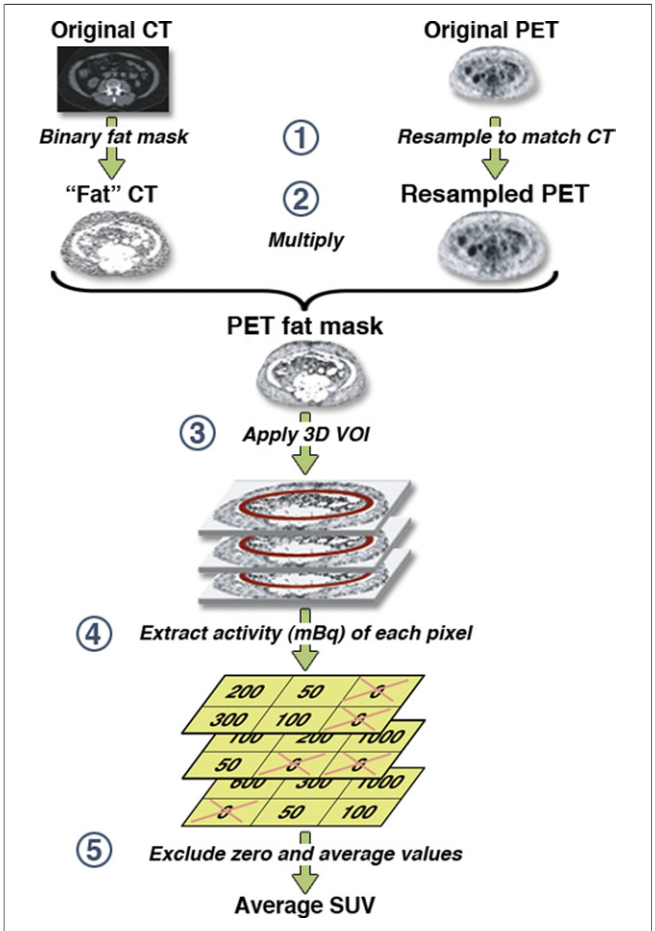

Figure 1. Flow Chart of FDG-PET/CT Image Analysis

(1) We created a binary "fat mask" of the computed tomography (CT) image by removing pixels with densities below −110 HU or above −70 HU. We resampled the positron emission tomography (PET) image to match slice thickness and the matrix size of the CT image. **(2)** We then multiplied the fat-masked CT image and resampled PET image to create a fat mask of the PET image. **(3)** We drew regions of interest on several slices and combined them to obtain a volume of interest (VOI). **(4)** We recorded tracer activity (becquerels per cubic centimeter) in each pixel and converted it to the standard uptake value (SUV). **(5)** We discarded 0 values and averaged all positive values to obtain an average SUV for the VOI. FDG = fluorodeoxyglucose.

Table 1. Sequences of Primers Used for RNA Amplification

Gene Name (GeneBank Accession #)	Forward Primer	Reverse Primer
GLUT-1 (NM_011400.3)	5′-ATGGATCCCAGCAGCAAG-3′	5′-CCAGTGTTATAGCCGAACTGC-3′
GLUT-3 (NM_011401.3)	5′-GGTGGCTGGCTGTTGTAACT-3′	5′-GCAGCGAAGATGATAAAAACG-3′
GLUT-4 (NM_009204.2)	5′-GACGGACACTCCATCTGTTG-3′	5′-GCCACGATGGAGACATAGC-3′
HK-1 (NM_010438.2)	5′-GCGAGGACAGGCTGTAGATG-3′	5′-CCGCATGGCATACAGATACTT-3′
HK-2 (NM_013820.3)	5′-CAACTCCGGATGGGACAG-3′	5′-CACACGGAAGTTGGTTCCTC-3′
GAPDH (XM_001473623.1)	5′-TGGGTGTGAACCATGAGAAG-3′	5′-GCTAAGCAGTTGGTGGTGC-3′

GAPDH = glyceraldehyde-3-phosphate dehydrogenase; GLUT = glucose transporter; HK = hexokinase.

mmol L-glutamine. We plated cells on 24-well plates at a density of 250,000 cells/well and allowed them to adhere for 24 h, after which we stimulated them with a mixture of murine TNF-alpha and IL-1beta (10 ng/ml each). We then performed glucose uptake in cultured cells at baseline and at 24 and 48 h after stimulation.

RNA isolation and analysis of gene expression. RNA isolation from the SVCs was performed using RNeasy mini spin columns (Qiagen, Germantown, Maryland), according to the manufacturer's instructions. We carried out RNA isolation from whole AT with RNeasy Lipid Tissue Midi Kit (Qiagen), according to the manufacturer's instructions. We assessed RNA concentration and purity using Nanodrop 1000 UV spectrophotometer (Thermo Scientific, Wilmington, Delaware). One microgram of RNA was reverse transcribed into complementary DNA (cDNA) using Superscript II reverse transcriptase (Invitrogen, Carlsbad, California) and oligo-dT primers (Invitrogen).

We performed quantitative polymerase chain reaction (qPCR) on 2 μl of cDNA with the MyiQ Real-Time PCR Detection System (BioRad, Hercules, California) using the primer sequences indicated in Table 1. We calculated relative expression ratios of genes in visceral fat compared with subcutaneous fat using the $\Delta\Delta$Cq method with GAPDH mRNA expression as reference. Further details on RNA isolation and qPCR can be found in the Online Methods supplement to the article.

Statistical analysis. We performed statistical analysis with the GraphPad Prism version 4.0 (GraphPad Software, La Jolla, California), StatView 5.0.1 (SAS Institute, Cary, North Carolina), and SAS version 9.1 (SAS Institute) software packages. Descriptive summaries included means, standard deviations, and percentages. The obese and lean cohorts were compared in terms of patient characteristics and fat SUV using the chi-square or Wilcoxon rank sum test. The within-subject analysis of VAT compared with SAT was a mixed models analysis of variance, with patient as a random effect and fixed effects of fat depot (SAT or VAT) and cohort (obese or lean). Potential confounding variables were added to the model individually, with each model having 3 fixed effects. Reliability of VAT and SAT SUV values in a subset of 8 obese and 8 lean patients was assessed by the Pearson correlation coefficient between the first and second repeated measures, the 95% confidence interval around the mean difference, and the intraclass correlation coefficient with 95% confidence interval. Statistical analysis on graphs 2 and 4 was performed using the Mann-Whitney *U* test, and the Wilcoxon signed rank test was used on graph 3. Nominal p values were reported, unadjusted for multiple testing.

RESULTS

We assessed FDG-PET scans from 31 obese (body mass index [BMI] >30 kg/m^2) and 26 lean (BMI <25 kg/m^2) subjects. Table 2 provides patient

Table 2. Baseline Characteristics of Patients

	Lean Patients (n = 26)	Obese Patients (n = 31)	p Value
Females	14 (54)	15 (48)	0.68
Age (yrs)	66.0 ± 14.8	61.4 ± 10.4	0.08
BMI (kg/m^2)	21.7 ± 0.6	36.4 ± 3.5	<0.001
Hypertension or antihypertensive drug	9 (35)	20 (65)	0.02
Diabetes	2 (8)	8 (26)	0.07
Smoking	15 (58)	14 (45)	0.35
CAD	2 (8)	7 (23)	0.12
Diuretic	3 (12)	8 (26)	0.17
Beta-blocker	5 (19)	9 (29)	0.39
Statin	2 (8)	7 (23)	0.12
Ca^{2+} blocker	1 (4)	5 (16)	0.13
ACE inhibitor	3 (12)	6 (19)	0.42
NSAID	6 (23)	7 (23)	0.96
Any drug	9 (35)	17 (55)	0.13

Values are n (%) or mean ± SD.
ACE = angiotensin-converting enzyme; BMI = body mass index; CAD = coronary artery disease; NSAID = nonsteroidal anti-inflammatory drug.

characteristics. There were significantly more obese patients with hypertension or on blood pressure medications, as compared with lean patients (65% vs. 35%, p = 0.02). The cohorts did not differ significantly in other patient characteristics.

Visceral fat in humans exhibits higher FDG uptake than subcutaneous fat. Analysis of FDG-PET/CT scans from patients revealed that lean and obese cohorts did not differ significantly with respect to subcutaneous FDG uptake (0.30 ± 0.09 vs. 0.33 ± 0.08, p = 0.18) or visceral FDG uptake (0.88 ± 0.18 vs. 0.81 ± 0.23, p = 0.15). Visceral fat showed significantly higher FDG uptake than subcutaneous abdominal AT in both the lean (BMI <25 kg/m^2) (p < 0.0001) and obese (BMI >30 kg/m^2) subjects (p < 0.0001) (Fig. 2). Potentially important covariates, such as age, sex, diabetes, a history of coronary artery disease, hypertension or use of antihypertensive therapy, and smoking history, did not affect this difference in FDG signal associated with fat depots. FDG uptake in SAT and VAT in men and women overall and within both lean and obese groups is shown in Online Figure 1. Medications (statins, diuretics, beta-adrenergic blockers, Ca^{2+}-channel blockers, angiotensin-converting enzyme inhibitors, and aspirin, or a combination of drugs) also did not alter results.

To investigate the reliability of the measurement, the assessment of FDG uptake was repeated in 8 obese and 8 lean patients. Table 3 shows mean differences and 95% confidence intervals around the mean differences, along with correlations and intraclass correlation coefficients. The measurements were most reliable for subcutaneous fat, with a correlation of 0.88 (p < 0.0001) and an intraclass correlation coefficient of 0.87 (95% confidence interval: 0.68 to 0.95).

To probe the mechanisms contributing to higher FDG uptake in visceral than in subcutaneous AT, we conducted a series of ex vivo and in vitro experiments on cells obtained from mouse AT.

2-Deoxy-glucose uptake is higher in mouse SVCs from visceral fat compared with subcutaneous fat. We first isolated SVCs from subcutaneous and visceral fat depots from mice with diet-induced obesity and measured glucose uptake in these cells. Baseline glucose uptake, normalized for protein content, was higher in SVCs from VAT compared with those from SAT (Fig. 3A). Interestingly, there were no apparent differences in the rate of glucose uptake in animals of different ages (data not shown). These findings corroborated our PET data in humans. SVCs from visceral fat also tended to show higher glucose uptake at 24 and 48 h after plating (Fig. 3A). TNF-alpha and IL-1beta, both important cytokines involved in AT inflammation, boosted glucose uptake in visceral and subcutaneous SVCs (Fig. 3B).

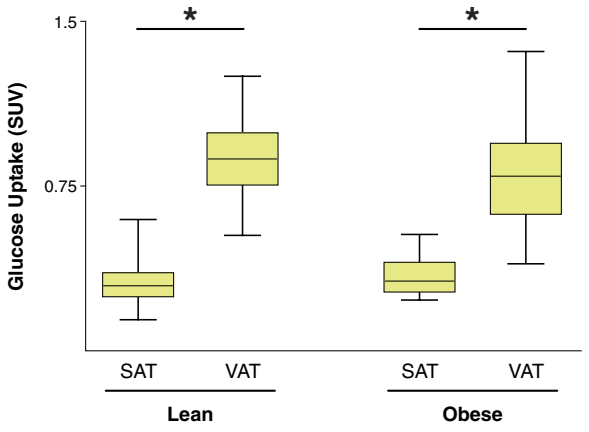

Figure 2. FDG Uptake in Human SAT and VAT

Average intensity of fluorodeoxyglucose (FDG) uptake (in standard uptake value [SUV]) in subcutaneous adipose tissue (SAT) and visceral adipose tissue (VAT) in lean patients (body mass index [BMI] between 21 and 22.7 kg/m^2) and obese patients (BMI between 32.8 and 45.3 kg/m^2). The **horizontal line** in the box plots represents the median value; the **boxed area** is the interquartile range, and the **whiskers** denote the 10th and 90th percentiles. *p < 0.05.

Expression of glucose metabolism-related genes in mouse AT. To examine further mechanisms that might increase glucose uptake in visceral fat, we studied the expression of glucose metabolism-related genes in mouse SVCs and unfractionated AT. We performed real-time PCR analysis for the expression of GLUT-1, -3, and -4, as well as HK-1 and 2, in SVCs isolated from SAT and VAT and in unfractionated AT from both depots. SVCs from VAT exhibited significantly higher expression of HK-1 compared with SVCs from SAT (Fig. 4A). This difference was observed in SVCs when data

Table 3. Evaluation of Reliability in Measurement of FDG Uptake

Group	Mean Difference (95% CI)	Correlation	ICC (95% CI)
Subcutaneous			
Overall	0.001 (−0.018, 0.019)	0.88, p < 0.0001	0.87 (0.68, 0.95)
Lean	0.010 (−0.018, 0.039)	0.93, p = 0.001	0.92 (0.72, 0.98)
Obese	−0.009 (−0.038, 0.021)	0.67, p = 0.07	0.67 (0.09, 0.91)
Visceral			
Overall	−0.065 (−0.15, 0.021)	0.60, p = 0.01	0.56 (0.13, 0.81)
Lean	−0.028 (−0.158, 0.102)	0.56, p = 0.15	0.59 (−0.04, 0.88)
Obese	−0.102 (−0.242, 0.039)	0.70, p = 0.05	0.53 (−0.13, 0.86)

CI = confidence interval; FDG = fluorodeoxyglucose; ICC = intraclass correlation coefficient.

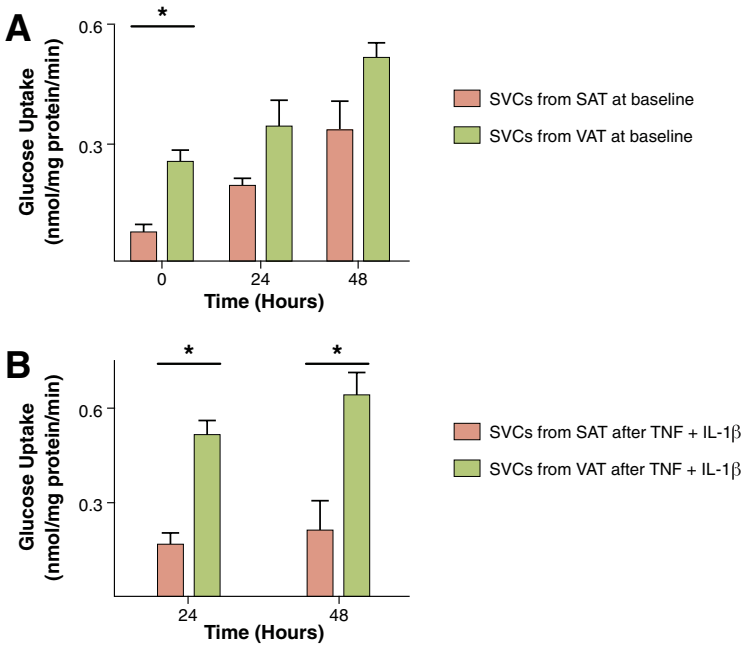

Figure 3. Glucose Uptake in SAT- and VAT-Derived SVCs

(A) Rate of glucose uptake in stromal vascular cells (SVCs) isolated from mouse subcutaneous adipose tissue (SAT) **(red bars)** and visceral adipose tissue (VAT) **(green bars)**. Glucose uptake is shown at baseline (0 h) and after 24 and 48 h of culture. Data are shown as mean ± SEM of 3 to 7 measurements. **(B)** Rate of glucose uptake in SVCs from SAT **(red bars)** and VAT **(green bars)** stimulated with inflammatory cytokines TNF-α and IL-1β for 24 and 48 h. Data are shown as mean ± SEM of 6 independent experiments. Cells obtained from subcutaneous depot were pooled from 2 to 3 animals. *$p < 0.05$.

were pooled from both 8-week-old and 16-week-old mice (Fig. 4) or analyzed separately at each age (data not shown). Levels of mRNAs encoding GLUT-1, -3, and -4 were lower in SVCs from visceral fat compared with SVCs from subcutaneous fat, but these differences were of much lesser magnitude than that of HK-1 induction (Fig. 4A). Real-time PCR on whole-fat samples from mice also revealed increased HK-1 expression in visceral compared with subcutaneous AT (Fig. 4B).

DISCUSSION

Physiologic differences between AT compartments in the body, particularly between subcutaneous and visceral depots, have long attracted attention. VAT burden portends higher cardiometabolic risk (4,5), whereas an increased amount of SAT shows the opposite association in obese individuals (6). Biologically, the 2 adipose depots also differ in the spectrum of inflammatory mediators they secrete.

This study tested the hypothesis that noninvasive functional imaging could reveal metabolic differences between AT depots in intact humans. Most clinical studies to date have used volumetric quantification of AT depots by CT or magnetic resonance imaging. A recent preliminary report, however, suggested that volumetric measurements alone may not be sufficient and could be improved with a functional readout of the metabolic activity in a fat compartment by means of PET (11). This report, however, did not investigate whether PET can detect differences between VAT and SAT compartments.

We show that VAT exhibits higher FDG uptake compared with SAT in humans in vivo. This difference remains significant after adjustment for potentially confounding covariates (age, sex, BMI, concomitant medications, or comorbidities including established diabetes, coronary artery disease, or hypertension) in the multivariate analysis. Thus, VAT displays higher metabolic activity than SAT, as assessed noninvasively in humans. Our results agree with earlier studies by Virtanen et al. (9,10), which showed higher rates of glucose uptake in VAT compared with SAT in groups of healthy and diabetic men under euglycemic hyperinsulinemic conditions. Although well designed, these studies enrolled only males with or without diabetes and did not assess basal rates of glucose uptake (9), which might limit the applicability of results to the general population. Our

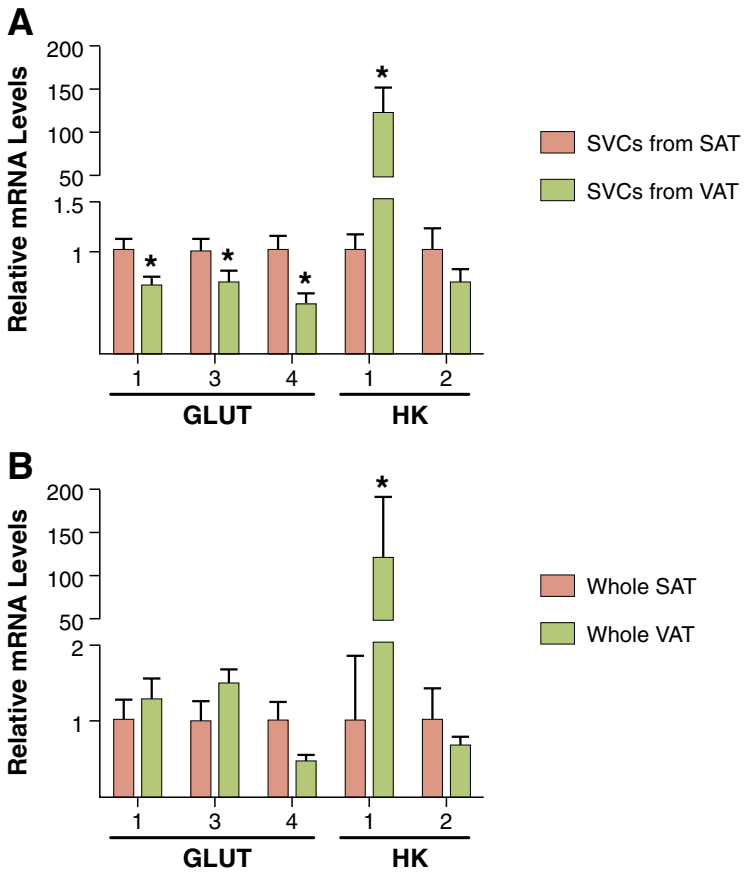

Figure 4. Expression of Glucose Metabolism-Related Genes in SAT and VAT

Expression of glucose metabolism-related mRNAs in stromal vascular cells (SVCs) **(A)** and in unfractionated adipose tissue **(B)** isolated from murine subcutaneous adipose tissue (SAT) and visceral adipose tissue (VAT). Gene expression in VAT-derived SVCs or unfractionated VAT (**green bars in A and B**, respectively) is shown relative to SAT-derived SVCs or unfractionated SAT (**red bars in A and B**, respectively) and normalized to housekeeping gene expression (GAPDH). Data are shown as mean ± SEM. *$p < 0.05$. GLUT = glucose transporter; HK = hexokinase.

study complements these results by assessing basal rates of glucose uptake in a heterogeneous group of subjects including both sexes, with or without comorbidities. Taken together, these results suggest that FDG-PET could enable noninvasive functional in vivo analysis of AT metabolic activity.

The clinical findings prompted a search for possible causes of different metabolic activity in SAT and VAT. In light of previous studies showing the presence of inflammatory cells in AT (15,16), we hypothesized that these cells may contribute to differential glucose uptake in VAT and SAT. SVCs derived from AT contain inflammatory cells such as macrophages and T cells. Indeed, VAT-derived SVCs isolated from diet-induced obese C57BL/6 mice exhibited significantly higher absolute rates of glucose uptake than those from SAT. We normalized glucose uptake values for protein concentration, which suggests increased rates of glucose uptake per cell of VAT rather than an increase due to greater cellularity in VAT. These findings indicate that not only increased cellularity, but also greater glucose uptake in each cell, contributes to the higher glucose uptake detected in vivo in human VAT compared with SAT.

Finally, to identify molecular mechanisms underlying differential glucose uptake in VAT and SAT, we assessed the expression of genes involved in the transport and phosphorylation of glucose. GLUTs mediate cellular uptake of this sugar (17). Upon entering the cell, glucose undergoes phosphorylation by hexokinase (HK), which exists in 2 main isoforms (HK-1 and HK-2) exhibiting different tissue localization (18). VAT-derived SVCs show higher HK-1 expression than SAT-derived SVCs. At the same time, expression of GLUT-1, -3, and

-4 was lower in VAT-derived SVCs, but exhibited much smaller differences between SAT- and VAT-derived SVCs, which raises questions regarding their biological contribution to the differences observed in glucose uptake. Moreover, HK-1 expression was also higher in unfractionated VAT compared with SAT, whereas GLUT-1, -3, and -4 and HK-2 expression levels did not differ. This suggests that the reduced expression of GLUT-1, -3, and -4 and HK-2 in SVCs within the VAT may be compensated by their higher level of expression in non-SVCs in the same fat pad. Therefore, the increase in HK-1 expression may be sufficient to increase glucose uptake in VAT and likely results from accentuated differences in expression in the SVCs. Perrini et al. (8) likewise showed that GLUT-1 and -4 expression did not differ between VAT and SAT SVC-derived adipocytes. These observations suggest that an increase in HK-1 expression may be sufficient to increase glucose uptake in VAT, as detected noninvasively by FDG-PET. Additional studies are nevertheless necessary to draw definitive conclusions.

Despite the association of obesity with inflammation, this study found no difference in FDG uptake in VAT between obese and lean individuals. We conjecture that even though SVCs in VAT from obese individuals contain more inflammatory cells, which could augment glucose uptake in VAT from obese subjects, their contribution to overall glucose uptake in such individuals may be counterbalanced by the greater mass of presumably insulin-resistant adipocytes, the most abundant cell type within this tissue.

Study limitations. We quantified FDG uptake in AT using SUVs, a clinically accepted way of analyzing PET studies. Nonetheless, SUVs may have intersubject and intrasubject variability as a result of multiple factors, including plasma glucose and insulin concentrations and the time of image acquisition after FDG injection. Moreover, quantification of FDG uptake requires 4-compartment kinetic analysis (19,20). Such analysis was not performed in our study, and therefore, our measurements are semiquantitative in nature.

CONCLUSIONS

We demonstrated significant differences in metabolic activity between SAT and VAT in humans using a standard noninvasive FDG-PET technique. Investigating mechanisms underlying this observation, we found increased glucose uptake in SVCs from VAT compared with SVCs from SAT in diet-induced obese mice. Further, we showed that the increase in glucose uptake in VAT may arise, in part, to increased expression of HK-1 in VAT-derived SVCs. These results affirm that different fat depots associated with distinct clinical outcomes exhibit differential metabolic activity in situ in intact humans.

Visceral adiposity has become a therapeutic target for numerous novel pharmacologic and other strategies aimed at the improvement of dysmetabolism. Although plasma biomarkers provide 1 window on efficacy, availability of an imaging modality to directly probe the target tissue would help drug development programs evaluate efficacy and perform better dose selection in clinical trials. These examples illustrate potential practical applications for the use of imaging adipose tissue metabolic activity.

Acknowledgments

The authors thank Jon Hainer from Brigham and Women's Hospital (Boston, Masschusetts), and Richard E. Lewis from Hermes Medical Solutions Inc., for their help with PET-CT image analysis. The authors also thank Elissa Simon-Morrissey for administrative assistance, and Sara Karwacki for editorial assistance.

Reprint requests and correspondence: Dr. Peter Libby, Cardiovascular Division, Department of Medicine, Brigham and Women's Hospital, Harvard Medical School, 77 Avenue Louis Pasteur, Boston, Massachusetts 02115. *E-mail: plibby@rics.bwh.harvard.edu.*

REFERENCES

1. Rosamond W, Flegal K, Furie K, et al. Heart disease and stroke statistics—2008 update: a report from the American Heart Association Statistics Committee and Stroke Statistics Subcommittee. Circulation 2008;117:e25–146.
2. Van Gaal LF, Mertens IL, De Block CE. Mechanisms linking obesity with cardiovascular disease. Nature 2006; 444:875–80.
3. Despres JP, Lemieux I. Abdominal obesity and metabolic syndrome. Nature 2006;444:881–7.
4. Canoy D, Boekholdt SM, Wareham N, et al. Body fat distribution and risk of coronary heart disease in men and women in the European Prospective Investigation Into Cancer and Nutrition in Norfolk cohort: a population-based prospective study. Circulation 2007; 116:2933–43.
5. Rosito GA, Massaro JM, Hoffmann U, et al. Pericardial fat, visceral abdominal fat, cardiovascular disease risk factors, and vascular calcification in a community-based sample: the Framingham Heart Study. Circulation 2008;117:605–13.

6. Porter SA, Massaro JM, Hoffmann U, Vasan RS, O'Donnel CJ, Fox CS. Abdominal subcutaneous adipose tissue: a protective fat depot? Diabetes Care 2009;32:1068–75.
7. Westergren H, Danielsson A, Nystrom FH, Stralfors P. Glucose transport is equally sensitive to insulin stimulation, but basal and insulin-stimulated transport is higher, in human omental compared with subcutaneous adipocytes. Metabolism 2005;54:781–5.
8. Perrini S, Laviola L, Cignarelli A, et al. Fat depot-related differences in gene expression, adiponectin secretion, and insulin action and signalling in human adipocytes differentiated in vitro from precursor stromal cells. Diabetologia 2008;51:155–64.
9. Virtanen KA, Lonnroth P, Parkkola R, et al. Glucose uptake and perfusion in subcutaneous and visceral adipose tissue during insulin stimulation in nonobese and obese humans. J Clin Endocrinol Metab 2002;87:3902–10.
10. Virtanen KA, Iozzo P, Hallsten K, et al. Increased fat mass compensates for insulin resistance in abdominal obesity and type 2 diabetes: a positron-emitting tomography study. Diabetes 2005;54:2720–6.
11. Brunken R, Freire M, Neumann D. Visceral fat volume is unrelated to adipose tissue inflammation (abstr). J Nucl Cardiol 2008;15:S7.
12. Britz-Cunningham SH, Millstine JW, Gerbaudo VH. Improved discrimination of benign and malignant lesions on FDG PET/CT, using comparative activity ratios to brain, basal ganglia, or cerebellum. Clin Nucl Med 2008;33:681–7.
13. Yoshizumi T, Nakamura T, Yamane M, et al. Abdominal fat: standardized technique for measurement at CT. Radiology 1999;211:283–6.
14. Kletzien RF, Perdue JF, Springer A. Cytochalasin A and B. Inhibition of sugar uptake in cultured cells. J Biol Chem 1972;247:2964–6.
15. Weisberg SP, McCann D, Desai M, Rosenbaum M, Leibel RL, Ferrante AW Jr. Obesity is associated with macrophage accumulation in adipose tissue. J Clin Invest 2003;112:1796–808.
16. Rocha VZ, Folco EJ, Sukhova G, et al. Interferon-gamma, a Th1 cytokine, regulates fat inflammation: a role for adaptive immunity in obesity. Circ Res 2008;103:467–76.
17. Uldry M, Thorens B. The SLC2 family of facilitated hexose and polyol transporters. Pflugers Arch 2004;447:480–9.
18. Wilson JE. Isozymes of mammalian hexokinase: structure, subcellular localization and metabolic function. J Exp Biol 2003;206:2049–57.
19. Hallett WA. Quantification in clinical fluorodeoxyglucose positron emission tomography. Nucl Med Commun 2004;25:647–50.
20. Castell F, Cook GJ. Quantitative techniques in 18FDG PET scanning in oncology. Br J Cancer 2008;98:1597–601.

Key Words: adipose tissue ■ adipocytes ■ stromal vascular cells ■ fluorodeoxyglucose ■ positron emission tomography ■ glucose uptake ■ inflammation.

▶ APPENDIX

For an expanded Methods section and a supplemental figure, please see the online version of this article.